Structural characterization and magnetic profile of annealed $CoFeB/MgO$ multilayers

M. Vadalá' , K. Zhernenkov, M. Wolff, B. P. Toperverg, K. Westerholt, H. Zabel, P. Wisniowski' , S. Cardoso, and P. P. Freitas

Citation: Journal of Applied Physics **105**, 113911 (2009); doi: 10.1063/1.3139281
View online: http://dx.doi.org/10.1063/1.3139281
View Table of Contents: http://aip.scitation.org/toc/jap/105/11
Published by the American Institute of Physics

Structural characterization and magnetic profile of annealed CoFeB/MgO multilayers

M. Vadalá,[1,a)] K. Zhernenkov,[1,2] M. Wolff,[1,2] B. P. Toperverg,[1,3] K. Westerholt,[1] H. Zabel,[1] P. Wisniowski,[4,b)] S. Cardoso,[4] and P. P. Freitas[4]
[1]*Experimentalphysik/Festkörperphysik, Ruhr-Universität Bochum, Universitätsstrasse 150, 44780 Bochum, Germany*
[2]*Institut Laue Langevin, rue Jules Horowitz, 38042 Grenoble, France*
[3]*Petersburg Nuclear Physics Institute, 188300 Gatchina, Russia*
[4]*INESC-Microsystems and Nanotechnologies, Rua Alves Redol 9, 1000-029 Lisboa, Portugal*

(Received 9 January 2009; accepted 28 April 2009; published online 3 June 2009)

Magnetic tunnel junctions (MTJ) have become of strategic importance due to the large tunneling magnetoresistance ratio (TMR) that they can achieve at room temperature. The largest TMR values observed until now were recorded in MTJs with MgO barriers and CoFeB electrodes after annealing of the junction above the recrystallization temperature of the amorphous CoFeB layers. We have used x-ray reflectivity combined with polarized neutron reflectivity to characterize the structure and the magnetism of $[Co_{60}Fe_{20}B_{20}/MgO]_{14}$ multilayers, where the MgO layers were prepared by different methods and annealed at different temperatures. We have found that the MgO preparation method as well as the annealing temperature play a significant role in the systems. A gradient in thickness together with a variation of the scattering length density along the multilayer stacks induce a process of underoxidation or overoxidation, strictly dependent on the MgO production method.
 [DOI: 10.1063/1.3139281]

I. INTRODUCTION

In recent years there has been a great deal of interest in using magnetic tunnel junctions (MTJs), which can achieve high tunnel magnetoresistance (TMR) ratios[1,2] for use in devices and sensors such as in nonvolatile magnetic random access memories and magnetic read heads of hard disk drives. The selection of materials used in a MTJ stack needs to be targeted at technological applications, usually requiring low switching fields, low saturation fields, and low device resistances.

Originally, most studies were devoted to MTJs with amorphous aluminium oxide barriers, yielding TMR ratios of 50%–70%. The TMR ratio is defined as the ratio $\Delta R/R_0$, where ΔR is the resistance change and $R_0(H)$ is the lowest resistance for a particular magnetic field H. The highest reported TMR ratio was 70% in MTJs using conventional $3d$ ferromagnetic metals such as Fe, Co, and Ni at room temperature.[3]

First-principles electronic structure calculations on fully ordered (001) oriented Fe/MgO/Fe MTJs suggested the possibility of TMR ratios of 100% to even 1000% for a sufficiently thick MgO barrier.[4,5] The TMR ratios of body centered cubic Co(001)/MgO(001)/Co(001) and the FeCo(001)/MgO(001)/FeCo(001) systems were predicted to be even higher by several times as compared to the TMR ratio predicted for the Fe/MgO/Fe system.[6] These giant TMR ratios are thought to be caused by an interfacial spin-dependent electronic state with Δ_1 symmetry at the Fermi energy.

Djavaprawira *et al.* [7] obtained results that are especially notable from the technological point of view because they deposited MTJs with standard spin-valve structure on thermally oxidized Si using a conventional sputtering method and then annealed them, obtaining a giant TMR ratio with amorphous CoFeB ferromagnetic electrodes.

Currently, the international focus in MTJ research is on CoFeB/MgO junctions, which in their amorphous state have the advantage to be homogenous at small scales, as required for high density recording media. To achieve large TMR values, these junctions must be annealed at temperatures between 250 and 360 °C. Annealing at 250 °C causes a partial crystallization of CoFeB, whereas annealing at higher temperatures (360–400 °C) leads to a full CoFeB recrystallization, independently of the Fe content in the alloy.

In this paper we present our results on structural and magnetic studies of $[Co_{60}Fe_{20}B_{20}/MgO]$ multilayers, grown on Si/SiO_2 substrates using three different processes for the preparation of the MgO layers. We observed changes of the structural quality of the multilayers after annealing at different temperatures. By means of x-ray reflectivity (XRR), we could investigate thickness fluctuations, multilayer periods, and interface roughness, whereas polarized neutron reflectivity was used to get insight about the magnetic layer properties and the magnetic depth profile.

II. PREPARATION AND EXPERIMENTAL

The CoFeB/MgO multilayers of this study have been prepared at INESC-MN (Lisbon, Portugal) by ion beam deposition, using $Co_{56}Fe_{24}B_{20}$ (at. %) and pure Mg metallic targets. We fully characterized three series of samples, annealed at different temperatures, where three methods to cre-

a)Author to whom correspondence should be addressed. Electronic mail: miriana.vadala@rub.de.
b)Present address: Siemens, Erlangen.

ate the MgO tunnel barrier were used. The samples were fabricated by ion beam deposition in a Nordiko 3600 system with a base pressure of 5×10^{-8} mbar.[8]

In the first series labeled as 1NAT the Mg film (1.6 nm thick) was oxidized in a natural flow of oxygen, 20 SCCM (SCCM denotes standard cubic centimeter per minute) O_2 flux for 120 s. In the second series labeled as 2REMOT, Mg was oxidized in an oxygen plasma environment, in 2 SCCM O_2 flux with Ar as inert gas for 45 s. The third series 3REACT was prepared by assisted deposition of the MgO layers from the Mg target, simultaneously with natural flow of oxygen, for 100 s. In the three cases, the oxygen and argon gas inlet was done using separate mass flow controllers, located at the assist gun (~75 cm away from the sample holder).

Within each series, different annealing temperatures were chosen to check the thermal stability, starting from the as-deposited state up to 360 °C. All samples were annealed for 2 h and protected with a Mg layer (3 nm), which oxidizes at contact with air. This cap layer was chosen to avoid the presence of extra materials in the x-ray spectra with the advantage of maintaining the same type of interfaces at the bottom and top layers in the multilayer stack.

The structural characterization of the multilayers has been carried out with synchrotron radiation ($E=h\nu$ =11.5 keV) at the beamline BL9 of the DELTA Synchrotron source at the University of Dortmund.[9] We have studied specular and (off specular) scattering in the small angle regime combining specular Q_z scans, longitudinal diffuse Q_z, and transverse diffuse Q_x scans (not shown here). The specular intensity was collected using standard θ-2θ scans along Q_z, where the z direction is defined by the growth direction. The true specular intensity, which is shown in the plots, has been obtained by subtracting the off-specular signal from the specular one.

Polarized neutron reflectivity (PNR) measurements have been performed using the ADAM reflectometer at the Institute Laue Langevin (ILL, Grenoble).[10,11] This instrument makes use of cold neutrons with wavelength $\lambda=0.441$ nm, which can be polarized and analyzed by transmission supermirrors. The initial polarization vector was directed either parallel or opposite to the ambient magnetic field. The latter was applied along the Y-axis, which is set within the plane of the sample surface and perpendicular to the reflection plane. The X-axis lies along the intersection between reflection and sample surface planes and hence perpendicular to the direction of the polarization analysis. In this geometry magnetization vector components parallel to the Y-axis do not alter the initial spin states and cause only non-spin-flip (NSF) scattering. The remaining magnetization components change spin states and cause spin-flip scattering. All x-ray and neutron data from the different samples were recorded at room temperature.

III. RESULTS AND DISCUSSION

A. Structural properties

In Fig. 1 we show XRR measurements performed at the DELTA Synchrotron source at the University of Dortmund[9] on samples of the series 1NAT, 2REMOT, and 3REACT all annealed at 280 °C. For 1NAT and 2REMOT, we observe fine film Kiessig fringes at least up to the first order Bragg peak and in some cases even beyond. Furthermore, multilayer Bragg peaks can be resolved up to the second order for the remotely oxidized multilayers and up to the third order for the naturally oxidized samples, indicating that the interfaces are relatively flat. For the 3REACT, only the first order peak is observed, indicating a much bigger degree of intermixing at the interfaces. This may be explained by the CoFeB oxidation during the Mg assisted deposition in the oxygen atmosphere.

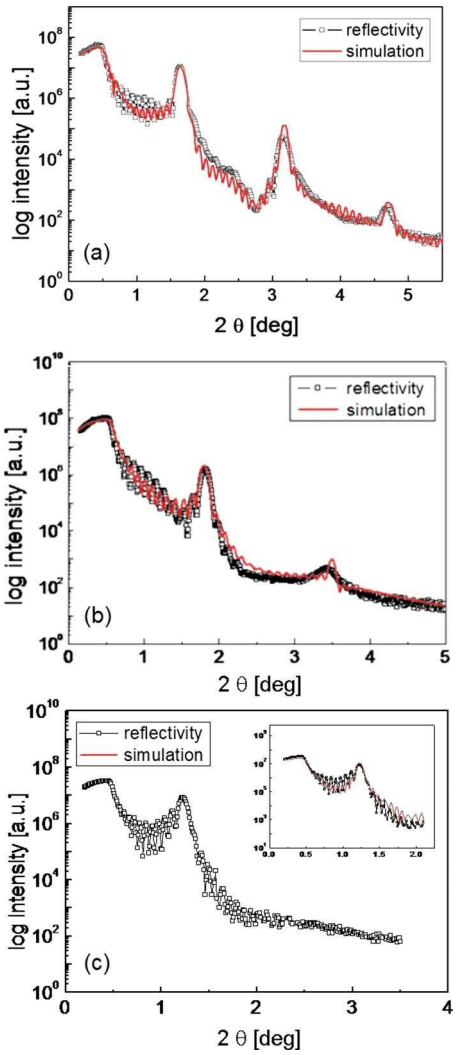

FIG. 1. (Color online) XRR curves and simulations for the mutlilayers $[CoFeB(3\ nm)/MgO(1.6\ nm)]_{14}$ 1NAT (a), 2REMOT (b), and 3REACT (c), annealed at 280 °C. Due to the higher degree of intermixing at the interfaces, we observed for 3REACT only the first Bragg peak (c). We could not fit the curve entirely. The fit around the first order Bragg peak is shown in the inset of (c).

In order to obtain reliable quantitative information on thicknesses and interface roughness parameters we have simulated the XRR data using the WINGXA code (Philips), which applies a genetic algorithm to adapt the model structure to the experimental data by an iterative process and the GENX software.[12] The experimental parameters resulting from the fit to the reflectivity curves of 1NAT and 2REMOT are listed in Table I. It was not possible to fit 3REACT with any reliability.

TABLE I. Nominal and experimental values obtained by the fit for the thickness and the roughness of the samples 1NAT and 2REMOT.

Sample ID	Bilayer thickness (nm)		Roughness (nm)	
	Nominal	Fit	CoFeB	MgO
1NAT (as deposited)	4.6	4.28	0.5	0.6
1NAT (annealed 280 °C)	4.6	4.12	0.5	0.4
1NAT (annealed 360 °C)	4.6	4.05	0.4	0.5
2REMOT (as deposited)	4.6	3.78	0.6	1.4
2REMOT (annealed 280 °C)	4.6	3.7	0.7	1.7
2REMOT (annealed 360 °C)	4.6	3.7	0.7	1.9

The interface roughness of the MgO layers is definitely smaller for the multilayer prepared by natural oxidation than for the plasma oxidation. Moreover, for the natural oxidation, the annealing hardly affects the mean square roughness parameter, whereas for the plasma oxidized samples the roughness parameter increases upon annealing. This indicates that interdiffusion or interface roughness upon annealing increases more strongly for plasma oxidized than for natural oxidized MgO layers. Interdiffusion might destroy the insulating property of the barrier and must be avoided in the preparation process of MTJs. Although with specular XRR we can not distinguish between roughness and interdiffusion, the reflectivity results indicate that natural oxidation should be the superior technique for preparing high quality MgO barriers in MTJs, withstanding a high temperature annealing step.

The bilayer thickness determined from the XRR listed in Table I shows a notable temperature dependence. Upon annealing the bilayers shrink, more dramatically in the naturally oxidized sample by about 5% after annealing at 360 °C than in the plasma oxidized sample (2.5%). This shrinking of the bilayer period must in part be attributed to the increase of the density of the CoFeB layers in the crystalline state, which is typically of the order of 1%.

In Fig. 2 we plot the reflectivity curves of series 2REMOT, recorded after different increasing annealing temperatures. One notices that the annealing causes some changes in the XRR curves. From the as-deposited state up to $T=360$ °C the second Bragg peak becomes less intense and broader and the third Bragg peak is not visible anymore. This means that the multilayer structure is influenced by the annealing process through interdiffusion and/or roughening at the interfaces. If roughening is the reason, this might be due to recrystallization at higher temperature, which needs to be confirmed by high angle Bragg diffraction, shown in Fig. 3.

High angle x-ray scattering measurements for the samples 1NAT, 2REMOT, and 3REACT are shown in Fig. 3. The scans were taken with Cu $K\alpha$ radiation using a rotating anode x-ray generator. We selected these three samples to investigate the different growth features, not as function of the annealing temperature, but as function of the MgO deposition method. All samples plotted in Fig. 3 were grown on a silicon substrate (100) and annealed at $T=280$ °C. First we note that high angle Bragg peaks and satellite peaks do not exist and are not expected from this amorphous multilayer. This is similar to Co/a-Al_2O_3 multilayers,[13] which exhibit

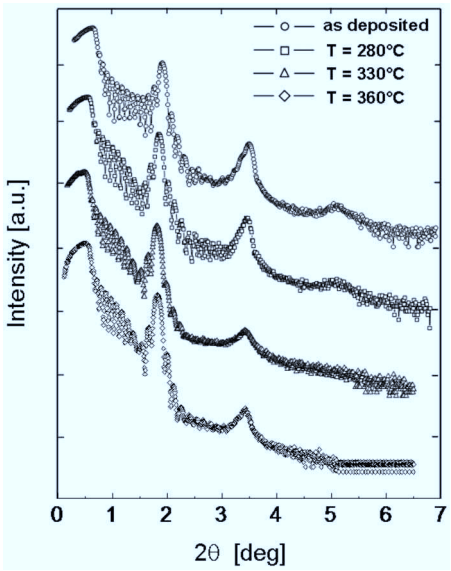

FIG. 2. Reflectivity curves for the samples 2REMOT, annealed at different increasing temperature.

many Bragg reflections at low angles from the multilayer periodicity but high angle superlattice Bragg peaks are absent due to the lack of lattice coherence. In the present case, we observe at $2\theta=47.3°$ a peak which is due to the Si (200) substrate. This peak is generally forbidden but may show some weak intensity via multiple beam Bragg reflection (Umweganregung).[14] More interesting features are observable at $2\theta=45°$, where the MgO (200) peak is present. This peak varies notably for the three samples. In particular it is more pronounced for sample 1NAT (natural oxidation), smaller and broader for sample 2REMOT (plasma remotely oxidized), and almost absent for sample 3REACT (reactively oxidized).

From the full width of the MgO (200) peak ΔQ at half maximum (FWHM) in Q ($=4\pi/\lambda \sin\theta$) scale we derive the out-of-plane coherence length of the multilayers using the equation $\xi=2\pi/\Delta Q$. The calculation yields for the structural coherence length ξ_{MgO} (1NAT)=14 nm, ξ_{MgO} (2REMOT) =12 nm, and ξ_{MgO} (3REACT)=11 nm. These values are more than twice as big as the nominal double layer periodicity of 4.6 nm. Our interpretation is that the MgO layers

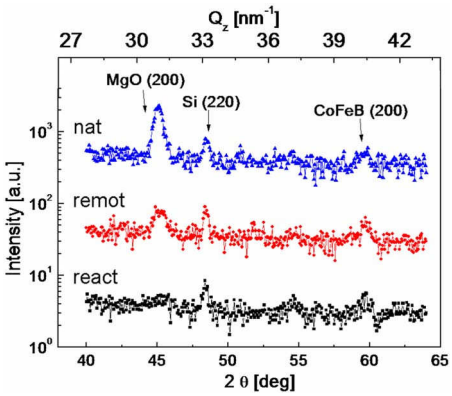

FIG. 3. (Color online) High angle x-ray θ-2θ scans for the multilayers 1NAT, 2REMOT, 3REACT all annealed at $T=280$ °C.

together with CoFeB form in small parts of the multilayer coherent and epitaxial stacks, whereas the majority of the sample is polycrystalline (MgO) and amorphous (CoFeB). These coherent stacks may serve as seeds for a more extended epitaxial recrystallization after annealing above 300 °C. We also notice a shift of the MgO (200) Bragg peak to higher 2θ values in the sequence from 1NAT to 3REACT. This shift is likely due to a variation of the oxygen concentration in the MgO layer. It appears that the correct stoichiometry is kept only for the sample naturally oxidized, where the peak is more pronounced. These results are also in agreement with those obtained by polarized neutron reflectivity.

Another peak is visible in all three scans at $2\theta=60°$. Assuming a bcc structure and neglecting the boron contribution this peak can be attributed to the CoFeB (200)reflection. For a completely amorphous CoFeB layer, this peak should be absent. Recrystallization is only expected for higher annealing temperatures. Thus this peak indicates that the magnetic layers may still contain some small crystalline grains after deposition. As discussed above, small crystalline grains may together with MgO form coherent stacks, penetrating through a few layers.

B. Polarized neutron reflectivity

We have performed PNR measurements on the same three multilayers annealed at 280 °C 1NAT, 2REMOT, and 3REACT that have already been analyzed with x-ray scattering. We chose these three multilayers to analyze how the different MgO production methods influence the magnetization profile within the CoFeB layers as well as the stoichiometry of the MgO layers. PNR is more sensitive to the oxygen concentration in MgO than XRR due to the large and almost equal coherent nuclear scattering length b of Mg (5.37 fm) and O (5.8 fm). In Fig. 4 we plot the neutron reflectivity curves for up-up, ($R++$), and down-down, ($R--$), NSF channels, taken at room temperature and in saturation of the CoFeB films ($H=400$ Oe). The large splitting between $R++$ and $R--$ is a clear sign for the magnetic state of the CoFeB layers, however, the details are quite different for the three samples. All three samples exhibit a bifurcation at the total reflection edge and a splitting of the $R++$ and $R--$ intensities of the total thickness oscillations. At the first multilayer Bragg peak, however, we observe a pronounced difference between the samples: in Fig. 4(a) for 1NAT the splitting between $R++$ and $R--$ vanishes; in Fig. 4(b) for 2REMOT $R++\gg R--$, where $R--$ is essentially distinct, and in Fig. 4(c) for 3REACT $R++<R--$. We can qualitatively explain the intensity variation, bearing in mind that the scattering length density (SLD), expressed as the product of the nuclear density and the coherent scattering length Nb, for stoichiometric MgO is accidentally very close to the nominal nuclear SLD value for $Co_{60}Fe_{20}B_{20}$, i.e., Nb (MgO) $\approx$ Nb ($Co_{60}Fe_{20}B_{20}$).

For this special case, the multilayer Bragg peaks vanish for a nonmagnetic sample. However, the total SLD is the sum of the nuclear and magnetic part: $Nb_{tot}=Np+Nb$. Thus, for polarized neutrons the intensity at the Bragg peaks is solely due to magnetic scattering. As CoFeB is ferromagnetic, the nuclear SLD of MgO Nb(MgO) is measured relative to the nuclear and magnetic SLD of CoFeB, Nb(CoFeB)+Np(CoFeB). If no difference is detected between the $R++$ and $R--$ reflectivity curves, then the magnetic contrast for up and down polarized neutrons is identical, which implies that the nuclear densities of the MgO and the CoFeB layers must match. If $R++>R--$ at the Bragg peak, MgO has a lower nuclear density than CoFeB, which is the case for sample 2REMOT. Vice versa, if $R++<R--$, the MgO density is higher than the CoFeB density, which is the case for sample 3REACT. Thus the scattering length densities for the MgO layers are different for the three preparation methods. Now, assuming that the naturally oxidized sample 1NAT has the correct value for the density of the MgO layer, in comparison sample 2REMOT has a smaller MgO density and sample 3REACT has a higher density. This argument is based on the reasonable assumption that the den-

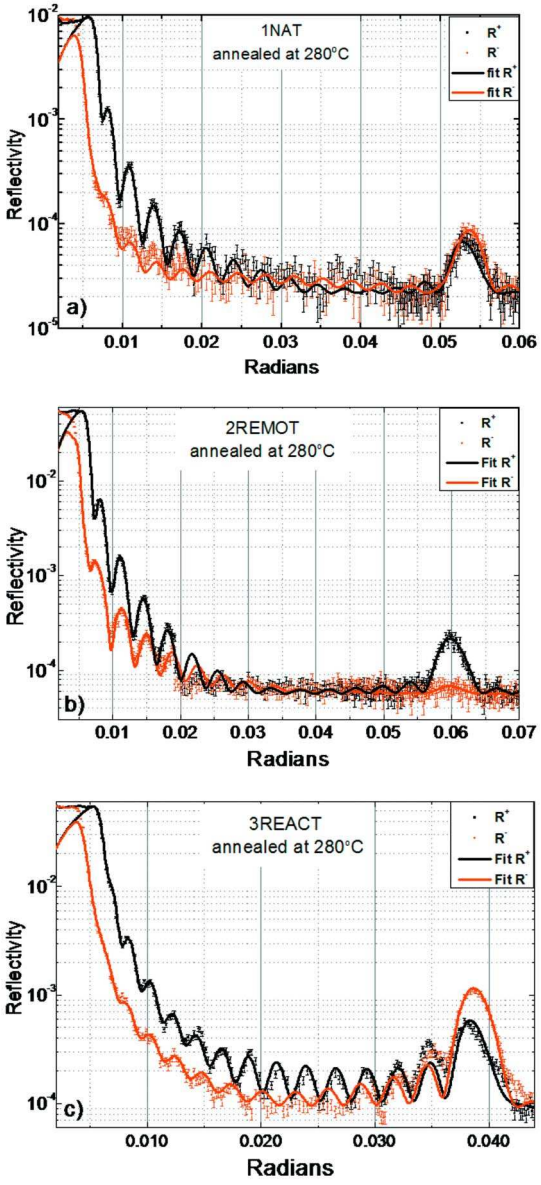

FIG. 4. (Color online) PNR $R++$ and $R--$ scans (points), together with the results (lines) of the fit to the theoretical model, for the multilayers 1NAT, 2REMOT, and 3REACT, all annealed at $T=280$ °C.

TABLE II. Experimental values obtained by the neutron fit for the thickness and the SLD of the samples 1NAT and 2REMOT and 3REACT annealed at 280 °C.

	Thickness (nm)		SLD (10^{-6} Å^{-2})		
Sample ID (annealed 280 °C)	Bilayer	MgO layer	CoFeB nuclear (Nb)	CoFeB Magnetic (Np)	MgO nuclear (Nb)
1NAT	4.15 ± 0.01	1.18 ± 0.04	4.90 ± 0.02	2.09 ± 0.03	5.09 ± 0.05
2REMOT	3.69 ± 0.03	0.29 ± 0.02	3.79 ± 0.02	2.38 ± 0.02	1.0 ± 0.3
3REACT	5.68 ± 0.02	1.94 ± 0.02	4.12 ± 0.01	1.80 ± 0.01	4.59 ± 0.01

sity of CoFeB is the same for all three samples. While with PNR measurements we clearly observe a density variation within the MgO layer, we cannot tell whether the density variation in MgO is due to Mg or to O. However, it seems plausible that a smaller density is connected with some oxygen deficiency and vacancies on the O sublattice whereas a larger density is connected with excess oxygen and some oxygen atoms on interstitial positions. Thus we infer that only the naturally oxidized MgO layers acquire the proper MgO density and the correct stoichiometry.

Quantitative analysis of the PNR data generally confirms the above consideration, adding details on the evolution of parameters of multilayers constructed under different procedures of magnesium oxidation. The results of the least square routine applied to the PNR data are listed in Table II. The fit quality can be judged from Fig. 4 where data are plotted together with the theoretical curves. Model reflectivity curves were convoluted with the instrumental resolution function, while experimental data at very low angles of incidence were excluded from the fit due to an appreciable background from the direct beam.

The best fit (lowest chi square) was obtained for the sample 1NAT, which exhibits a rather coherent structure throughout almost the whole multilayer stack. The bilayer thickness coincides remarkably well with the XRR results (see Table I) with quite high precision. Due to the more restricted Q range ($Q=4\pi/\lambda \sin\theta$) for PNR as compared to XRR, the interfacial roughness parameters were not determined. However, the PNR data provide the thickness on the MgO layer, as well as all SLD values for both layers and for the nuclear and magnetic part with a high degree of reliability. From these fits, we infer not only differences in the Mg oxidation procedures, but also the concentration of the bilayer constituents on an absolute scale. For instance, the value $\mathrm{Nb(CoFeB)}=4.90\times10^{-6}$ Å^{-2} determined for 1NAT is slightly higher than the nominal value $\mathrm{Nb}=4.51\times10^{-6}$ Å^{-2}, indicating that the concentration of iron and/or boron was actually higher than the expected 20% since both these elements have a much higher nuclear SLD [$\mathrm{Nb(Fe)}=8.09\times10^{-6}$ Å^{-2}, $\mathrm{Nb(B)}=7.57\times10^{-6}$ Å^{-2}] as compared to Co [$\mathrm{Nb(Co)}=2.27\times10^{-6}$ Å^{-2}]. On the other hand, the magnetic SLD of $\mathrm{Np(CoFeB)}=2.09\times10^{-6}$ Å^{-2} corresponds to a magnetization $M=9$ kOe, which is by 40% lower than the value $M=13$ kOe expected from magnetic measurements on corresponding bulk alloys of the same composition. A reduced magnetization can, in principle, be due to so called "magnetically dead" atomic layers of transition metals in contact with MgO. In our samples, such layers may be formed by partial oxidation of Fe and/or Co elements during oxidation procedure applied to transform Mg into MgO. For nonmagnetic oxides the nuclear SLD can be as high as $\mathrm{Nb(CoO)}=4.3\times10^{-6}$ Å^{-2} and $\mathrm{Nb(Fe_2O_3)}=7.26\times10^{-6}$ Å^{-2}. Therefore monoatomic interfacial layers containing CoO can reduce the average magnetic SLD by as much as 40%, while enhancing the nuclear SLD to the observed values. One should keep in mind that the present PNR data do not allow an unambiguous distinction between a reduction of the magnetic SLD due to nonmagnetic oxides at the interface and an enhanced boron concentration, which would also enhance the mean nuclear SLD while reducing the net magnetization of CoFeB.

Still remaining with the discussion of 1NAT, the SLD value $\mathrm{Nb(MgO)}=5.09\times10^{-6}$ Å^{-2} of the MgO layers is found to be appreciably lower than the nominal value $\mathrm{Nb(MgO)}=5.85\times10^{-6}$ Å^{-2} for bulk stoichiometric MgO, implying that the density of the MgO layer is reduced by about 15% compared to ideal MgO. On the other hand, one should keep in mind that the layer thickness is only 1.6 nm, i.e., a large fraction of the MgO film belongs to the interfacial regions on either side, where MgO is in contact with the metal layers.

Now we turn our discussion to the sample 2REMOT. The bilayer thickness determined by PNR for 2REMOT is again in excellent agreement with the XRR results. Moreover, the PNR fit results show that the MgO layer density is reduced by a factor of almost 6 [$\mathrm{Nb(MgO)}=10^{-6}$ Å^{-2}] as compared to the nominal value [$\mathrm{Nb(MgO)}=5.85\times10^{-6}$ Å^{-2}]. Such a huge reduction and small value can, however, be determined only with an accuracy of about 30%. This error bar is also due to minute MgO layer thicknesses of only 0.3 nm, which slightly exceeds the unit cell parameter. 2REMOT exhibits a relatively high value for the magnetic SLD of the metal layer [$\mathrm{Np(CoFeB)}=2.38\times10^{-6}$ Å^{-2}], whereas the nuclear SLD is lower than in 1NAT [$\mathrm{Nb(CoFeB)}=3.79\times10^{-6}$ Å^{-2}]. This is strongly indicative for an enhanced and nonoxidized Co concentration in this sample.

The quality of the data fit for the sample 3REACT is somewhat worse than for the other two samples. The fit is substantially improved by allowing an independent variation of the parameters for the two outermost pairs of layers at the top and bottom of the sample. This confirms the hypothesis based on XRR results that the multilayer period is not well preserved throughout the multilayer stack. The PNR data fit reliably shows that the magnetic SLD and hence the magnetization of the CoFeB layers is slightly lower than for the

1NAT sample. At the same time the nuclear SLD is higher than that of the 2REMOT sample. This requires a higher concentration of magnetic Co than that was found in the 1NAT case, whereas Co should be oxidized more than in the 2REMOT sample. On the other hand, the SLD value for the MgO layers [$Nb(MgO)=4.6\times10^{-6}$ Å^{-2}] is much higher than for 2REMOT but slightly less than for the 1NAT sample.

IV. SUMMARY AND CONCLUSIONS

Our x-ray and PNR results on $[Co_{60}Fe_{20}B_{20}/MgO]_{14}$ multilayers revealed that the interfaces between CoFeB and MgO are rather smooth and do not deteriorate noticeably when the sample is annealed at high temperatures. Some additional interdiffusion takes place at high annealing temperatures, especially for the samples where the MgO layers were prepared by plasma oxidation.

From the PNR data, we have determined the magnetization profiles for each of the three samples 1NAT, 2REMOT, and 3REACT studied after annealing at 280 °C. A sharp magnetization profile without signs of interdiffusion at this temperature was sufficient to describe the data. The magnetization of all samples is found to be substantially reduced with respect to the value of 1.3 T expected for the bulk amorphous alloy, with nominal concentrations for Co and Fe and magnetic moments expected from Slater–Pauling curve. Furthermore, we infer that the nuclear density of the MgO layers in the CoFeB/MgO multilayers definitely depends on the preparation method and on the MgO sputtering conditions. In all three cases, the MgO density turns out to be appreciably lower than that for single crystalline MgO. Our results suggest that only the naturally oxidized and assisted deposition of the MgO layers may come close to the correct stoichiometry. For the plasma oxidation method, the MgO density is found extremely low and may indicate some oxygen deficiency, resulting in an underoxidized samples; for the reactively sputtered MgO an overoxidation process most likely occurs extending towards the CoFeB films, which results in a reduced layer magnetization. High angle Bragg scattering reveals the presence of some small and coherent CoFeB/MgO crystallites, which may act as seeds during high temperature annealing steps.

As x-ray characterization of single MgO films prepared by these three methods did not show strong (002) texture, we microfabricated more than 100 different MTJ stacks to measure transport properties. We reached a maximum TMR of 20% when the Mg was naturally oxidized and less than 10% using remote plasma or reactive oxidation. Targeting at resistance areas in the $k\Omega/\mu m^2$ range, better results can be obtained using a ceramic MgO target, rather than with Mg plus oxidation.

In conclusion, we have analyzed by x-ray and PNR, the structure and magnetism of $[Co_{60}Fe_{20}B_{20}/MgO]_{14}$ multilayers, which are of high interest for MTJs. The crucial question to be answered by these scattering methods is which of the MgO preparation processes serves best for the fabrication of tunnel barriers: natural oxidation, remote oxidation, or reactive sputtering. With PNR measurements, we found large variations of the Mg:O stoichiometry depending on the growth mode, the natural oxidation being closest to the expected stoichiometry. The x-ray results confirmed that the recrystallization of MgO and the formation of a well defined texture does not take place to the extend expected. These studies indicate that the use of MgO targets for the tunnel barriers should be preferred over the deposition of Mg followed by some means of subsequent oxidation.

ACKNOWLEDGMENTS

The authors kindly acknowledge Dr. C. Sternemann and Dr. M. Paulus for their assistance during the experiments at the synchrotron source Delta, Dortmund and the financial support provided through the European Union's Marie Curie actions (Research Training Networks) ULTRASMOOTH under Contract No. MRTN-CT-2003-504462. The neutron work performed with the ADAM reflectometer at the Institut Laue-Langevin (Grenoble, France) was funded by Grant No. BMBF 03ZA7BOC.

[1] T. Miyazaki and N. Tezuka, J. Magn. Magn. Mater. **139**, L231 (1995).
[2] J. S. Moodera, L. R. Kinder, T. M. Wong, and R. Meservey, Phys. Rev. Lett. **74**, 3273 (1995).
[3] D. Wang, C. Nordman, J. Daughton, Z. Qian, and J. Fink, IEEE Trans. Magn. **40**, 2269 (2004).
[4] W. H. Butler, X.-G. Zhang, T. C. Schulthess, and J. M. MacLaren, Phys. Rev. B **63**, 054416 (2001).
[5] J. Mathon and A. Umersky, Phys. Rev. B **63**, 220403 (2001).
[6] X. G. Zhang and W. H. Butler, Phys. Rev. B **70**, 172407 (2004).
[7] D. D. Djayaprawira, K. Tsunekawa, M. Nagai, H. Maehara, S. Yamagata, N. Watanabe, S. Yuasa, Y. Suziki, and K. Ando, Appl. Phys. Lett. **86**, 092502 (2005).
[8] S. Cardoso, R. Macedo, R. Ferreira, A. Augusto, P. Wisniowski, and P. P. Freitas, J. Appl. Phys. **103**, 07A905 (2008).
[9] C. Krywka, M. Paulus, C. Sternemann, M. Volmer, A. Remhof, G. Nowak, A. Nefedov, B. Pöter, M. Spiegel, and M. Tolan, J. Synchrotron Radiat. **13**, 8 (2006).
[10] A. Schreyer, R. Siebrecht, U. Englisch, U. Pietsch, and H. Zabel, Physica B **248**, 349 (1998).
[11] M. Wolff, K. Zhernenkov, and H. Zabel, Thin Solid Films **515**, 5712 (2007).
[12] A. Leenaers and D. de Boer, X-Ray Spectrom. **26**, 115 (1997).
[13] C. Morawe and H. Zabel, J. Appl. Phys. **77**, 1969 (1995).
[14] R. Colella, Acta Crystallogr., Sect. A: Cryst. Phys., Diffr., Theor. Gen. Crystallogr. **30**, 413 (1974).